Available online at www.sciencedirect.com
ScienceDirect
Nuclear Instruments and Methods in Physics Research A 577 (2007) 86–92
NUCLEAR INSTRUMENTS & METHODS IN PHYSICS RESEARCH Section A
www.elsevier.com/locate/nima

Nonlinear δf particle simulations of collective effects in high-intensity bunched beams☆

Hong Qin*, Ronald C. Davidson, Edward A. Startsev

Princeton Plasma Physics Laboratory, Princeton University, Princeton, NJ 08543, USA

Available online 24 February 2007

Abstract

Collective effects with strong coupling between the longitudinal and transverse dynamics are of fundamental importance for applications of high-intensity bunched beams. The self-consistent Vlasov–Maxwell equations are applied to high-intensity bunched beams, and a generalized δf particle simulation algorithm is developed for bunched beams with or without energy anisotropy. Numerically, the distribution function is spit into a reference distribution and a perturbed part. The perturbed distribution function is represented as a weighted summation over discrete particles, where the particle orbits are advanced by the equations of motion in the focusing field and self-generated fields, and the particle weights are advanced by an equation equivalent to the nonlinear Vlasov equation. The nonlinear δf method exhibits minimal noise and accuracy problems in comparison with standard particle-in-cell simulations. Systematic studies are carried out for the particle dynamics under conditions corresponding to strong 3D nonlinear space-charge force. The simulations showed that finite bunch-length effects on the collective excitations become insignificant when the aspect ratio $(z_{\rm b}/r_{\rm b})$ is larger than 10 for a moderately intense beam with normalized intensity $s_{\rm b} = \omega_{p{\rm b}}^2/2\omega_\beta^2 = 0.27$. For bunched beams with energy anisotropy $(T_\parallel/T_\perp < 1)$, a reference state has been constructed and a dynamic equilibrium is established in the simulations. Collective excitations relative to the dynamic equilibrium have also been successfully simulated by the generalized δf algorithm.
Published by Elsevier B.V.

PACS: 29.27.Bd; 41.85.Ct; 41.85.Ew

Keywords: High-intensity beam; Bunched beam; Perturbative particle simulation

1. Introduction

Collective effects in high-intensity charged particle beams are often manifested as collective excitations with certain important dynamical properties such as instabilities and Landau damping. The self-consistent theoretical framework for studying the collective effects is provided by the nonlinear Vlasov–Maxwell equations [1]. A corresponding numerical method, the δf particle simulation method, has been developed [2] to solve the nonlinear Vlasov–Maxwell equations with significantly reduced noise. This theoretical and numerical framework has been successfully applied to study stable beam propagation [3], electron–ion two-stream (electron cloud) instabilities [4–6], and energy anisotropy instabilities [7,8]. However, previous studies were carried out for long coasting beams with arbitrary nonlinear space-charge intensity in the transverse direction. In this paper, we further develop the Vlasov–Maxwell equations and the δf simulation method to study collective effects for bunched beams with nonlinear space-charge fields in both the longitudinal and transverse directions.

Collective effects with strong coupling between the longitudinal and transverse dynamics are of fundamental importance for the applications of high-intensity bunched beams. For example, present accelerator research and development in the US Heavy Ion Fusion Science Virtual National Laboratory is focused on the capability of compressing an ion charge bunch both longitudinally and transversely to reach the high-intensity and short-pulse length required for creating high energy density matter and heavy ion fusion conditions in the laboratory. Collective

☆Supported by the U.S. Department of Energy.
*Corresponding author.
E-mail address: hongqin@princeton.edu (H. Qin).

0168-9002/$ - see front matter Published by Elsevier B.V.
doi:10.1016/j.nima.2007.02.038

effects associated with the longitudinal compression of bunched beams have not been systematically explored. For bunched beams, the equilibrium and collective excitation properties are qualitatively different from those for coasting beams. Especially, when the bunch length is compressed by a large factor, the coupling between the longitudinal and transverse dynamics induced by the 3D nonlinear space-charge fields become significant. A direct consequence of this coupling effect is that the particle dynamics does not conserve transverse energy and longitudinal energy separately, and there exists no exact kinetic equilibrium which has an anisotropic energy in the transverse and longitudinal directions. In this paper, we develop a reference state for beams with anisotropic energy, which is not an exact equilibrium solution of the Vlasov–Maxwell equation system. The difference between the exact solution and the reference state is simulated by a generalized δf particle simulation algorithm. If the beam is a thermal equilibrium distribution with isotropic energy, the reference state becomes an exact equilibrium solution, and the generalized δf particle simulation algorithm reduces to the conventional one. Even in this case, the particle trajectories on constant energy surfaces are nonintegrable [9,10], which implies that it is impossible to perform an integration along unperturbed orbits to analytically calculate the linear eigenmodes.

The paper is organized as follows. After the development of the generalized δf particle simulation algorithm in Section 2, the nonintegrability of the particle dynamics and collective excitations in bunched beams with energy isotropy are studied in Section 3. Then, in Section 4, the reference state and collective excitations for bunched beam with energy anisotropy are investigated.

2. Theoretical model and the generalized δf simulation method

To simplify the problem, in the present study we consider a single-species, bunched beam confined in both the r- and z-directions by an external smooth focusing force in the beam frame

$$\mathbf{F}_{\text{foc}} = -m\omega_\beta^2\mathbf{x}_\perp - m\omega_z^2 z\mathbf{e}_z. \tag{1}$$

Here, ω_β and ω_z are the constant transverse and longitudinal focusing frequencies in the smooth-focusing approximation. In the beam frame, the dynamics of the bunched beam is described by the nonlinear Vlasov–Maxwell equations [1]

$$\left\{\frac{\partial}{\partial t} + \mathbf{v}\cdot\frac{\partial}{\partial \mathbf{x}} - \left[m(\omega_\beta^2\mathbf{x}_\perp + \omega_z^2 z\mathbf{e}_z) + e\left(\nabla\phi - \frac{v_z}{c}\nabla_\perp A_z\right)\right]\cdot\frac{\partial}{\partial \mathbf{p}}\right\} f(\mathbf{x},\mathbf{p},t) = 0 \tag{2}$$

$$\nabla^2\phi = -4\pi e\int \mathrm{d}^3p f(\mathbf{x},\mathbf{p},t) \tag{3}$$

$$\nabla^2 A_z = -\frac{4\pi}{c} e\int \mathrm{d}^3p v_z f(\mathbf{x},\mathbf{p},t) \tag{4}$$

where e and m are the particle charge and rest mass, respectively.

This set of equations is a simplified version of the nonlinear Vlasov–Maxwell equations in the general case [1,6]. For the boundary conditions, a perfectly conducting cylindrical pipe is located at radius $r = r_\mathrm{w}$. To numerically solve the Vlasov–Maxwell equations, we use the low-noise δf method [2,4,5], where the total distribution function is divided into two parts, $f = f_0 + \delta f$. Here, f_0 is a *known* reference distribution function and the numerical simulation is carried out to determine the detailed nonlinear evolution of the perturbed distribution function δf. This is accomplished by advancing the weight function defined by $w \equiv \delta f/f$, together with the particles' positions and momenta. The dynamical equation for w is given by

$$\frac{\mathrm{d}w}{\mathrm{d}t} = -(1-w)\frac{1}{f_0}\left[\left(\frac{\mathrm{d}f_0}{\mathrm{d}t}\right)_\delta + \left(\frac{\mathrm{d}f_0}{\mathrm{d}t}\right)_0\right] \tag{5}$$

$$\left(\frac{\mathrm{d}f_0}{\mathrm{d}t}\right)_\delta = -e\left(\nabla\delta\phi - \frac{v_z}{c}\nabla_\perp\delta A_z\right)\cdot\frac{\partial f_0}{\partial\mathbf{p}} \tag{6}$$

$$\left(\frac{\mathrm{d}f_0}{\mathrm{d}t}\right)_0 = \left\{\frac{\partial}{\partial t} + \mathbf{v}\cdot\frac{\partial}{\partial \mathbf{x}} - \left[m(\omega_\beta^2\mathbf{x}_\perp + \omega_z^2 z\mathbf{e}_z) + e\left(\nabla\phi_0 - \frac{v_z}{c}\nabla_\perp A_{z0}\right)\right]\cdot\frac{\partial}{\partial \mathbf{p}}\right\} f_0 \tag{7}$$

where $\delta\phi \equiv \phi - \phi_0$, and $\delta A_z \equiv A_z - A_{z0}$. For the perturbed fields, Maxwell's equations are

$$\nabla^2\delta\phi = -4\pi e\int \mathrm{d}^3p\, w f(\mathbf{x},\mathbf{p},t) \tag{8}$$

$$\nabla^2\delta A_z = -\frac{4\pi}{c} e\int \mathrm{d}^3p v_z w f(\mathbf{x},\mathbf{p},t). \tag{9}$$

Here, the reference potentials (ϕ_0, A_{z0}) are chosen to satisfy

$$\nabla^2\phi_0 = -4\pi e\int \mathrm{d}^3p f_0(\mathbf{x},\mathbf{p},t) \tag{10}$$

$$\nabla^2 A_{z0} = -\frac{4\pi}{c} e\int \mathrm{d}^3p v_z f_0(\mathbf{x},\mathbf{p},t). \tag{11}$$

Of course, it is desirable to pick $(\phi_0,\ A_{z0},\ f_0)$ as self-consistent solutions to the Vlasov–Maxwell equations (2)–(4), such that the $(\mathrm{d}f_0/\mathrm{d}t)_0$ term in Eq. (5) vanishes. For most applications, $(\phi_0,\ A_{z0},\ f_0)$ are chosen to correspond to an equilibrium solution with $\partial/\partial t = 0$. However, for beams with energy anisotropy, exact equilibrium solutions do not exist due to the lack of invariants of the particle dynamics. Therefore, we can only choose a reference distribution f_0 that is close to an equilibrium solution. If the beam is isotropic in energy, the reference state can be chosen to be an exact equilibrium solution, and the generalized δf particle simulation algorithm reduces to the conventional nonlinear δf method

[5]. For a single-species beam, we neglect A_z in the beam frame because $|A_z| \ll |\phi|$.

3. Collective excitations for bunched beams with isotropic energy

Since the conventional concept of collective excitations or eigenmodes of charged particle beams refers to perturbations around a self-consistent equilibrium, the first step in this investigation is to identify possible equilibrium solution (ϕ_0, f_0) with $\partial/\partial t = 0$ satisfying

$$\left\{\mathbf{v}\cdot\frac{\partial}{\partial\mathbf{x}} - [m(\omega_\beta^2\mathbf{x}_\perp + \omega_z^2 z\mathbf{e}_z) + e\nabla\phi_0]\cdot\frac{\partial}{\partial\mathbf{p}}\right\} f_0(\mathbf{x},\mathbf{p}) = 0 \quad (12)$$

$$\nabla^2\phi_0 = -4\pi e\int \mathrm{d}^3p f_0(\mathbf{x},\mathbf{p}). \quad (13)$$

Eq. (12) implies that f_0 is an invariant of the particle dynamics in the equilibrium space-charge potential ϕ_0 and the external focusing field. Therefore, f_0 is a function of all of the independent invariants. Even for the simple model adopted here for bunched beams, there are only two invariants of the single particle dynamics in the equilibrium field, the total energy H and canonical angular momentum P_θ defined by

$$H = \frac{p^2}{2m} + e\phi_0 + \frac{1}{2}m(\omega_\beta^2 r^2 + \omega_z^2 z^2) \quad (14)$$

$$P_\theta = rmv_\theta. \quad (15)$$

In this section, we choose f_0 to be a function of H only according to

$$f_0 = f_0(H) = \frac{\hat{n}}{(2\pi mT)^{3/2}}\exp\left(\frac{-H}{T}\right) \quad (16)$$

which gives an isotropic temperature $T = \text{const}$. Here, $\hat{n}$ is the beam number density at $(r,z) = (0,0)$. Under this assumption, the equilibrium Poisson equation (13) becomes

$$\nabla^2\phi_0 = -4\pi e\hat{n}\exp\left[-\frac{m(\omega_\beta^2 r^2 + \omega_z^2 z^2)}{2T} - \frac{e\phi_0}{T}\right] \quad (17)$$

which can be solved numerically for ϕ_0 in a perfect cylindrical conducting pipe with wall radius $r = r_w$. It can be shown [1] that the condition for the beam being confined by the focusing field is

$$s_b \leqslant 1 + \frac{\omega_z^2}{2\omega_b^2}. \quad (18)$$

Here, $s_b \equiv 4\pi\hat{n}e^2/2m\omega_\beta^2$ measures the relative strength of the space-charge force compared with the applied focusing force in the transverse direction. Even though the kinetic equilibrium is taken to be the well-behaved thermal equilibrium in Eq. (16), the dynamics of a single particle on the constant energy surface is nonintegrable due to the coupling between the transverse and longitudinal dynamics induced by the 3D nonlinear space-charge force [10]. The coupling is a function of the space-charge strength and the bunch length. When the space charge intensity is reduced to zero, or the bunch length is increased to infinity, the transverse and longitudinal space-charge forces decouple and the particle dynamics is integrable.

As an example, we consider a bunched beam with $s_b = 1.1$ and $\omega_z/\omega_\beta = 0.50$. Eq. (17) is numerically solved for ϕ_0. Plotted in Fig. 1 is the normalized equilibrium density as a function of (r,z),

$$\frac{n_0}{\hat{n}} \equiv \exp\left[\frac{-m(\omega_\beta^2 r^2 + \omega_z^2 z^2)}{2T} - \frac{e\phi_0}{T}\right]. \quad (19)$$

Fig. 2shows the $r-v_r$ Poincaré plot at $z=0$ for particles with normalized energy $H/T = 1$ and normalized canonical angular momentum $P_\theta\omega_\beta/T = 0.25$. The formation of multiple islands of different scale-length in the $r-v_r$ Poincaré plot indicates the coupling between the

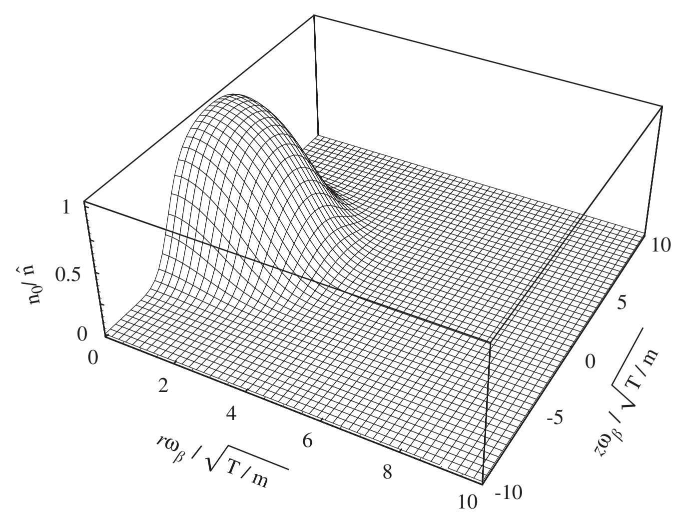

Fig. 1. Equilibrium beam density at a function of (r,z) for a bunched beam with $s_b = 1.1$.

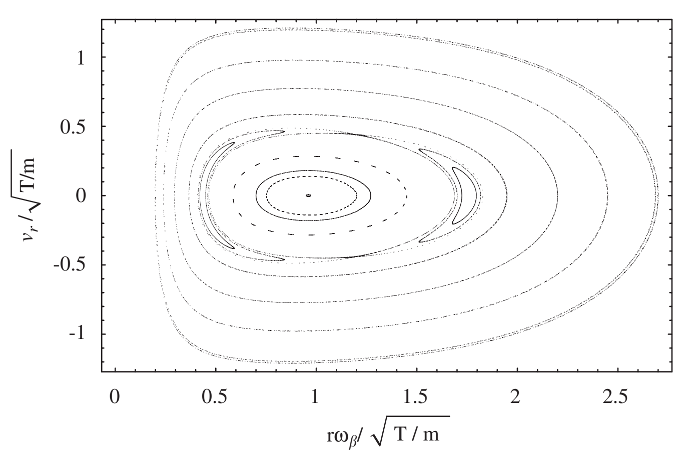

Fig. 2. The $r-v_r$ Poincaré plot at $z=0$ with constant energy and canonical angular momentum in a bunched beam with $s_b = 1.1$.

longitudinal and transverse dynamics. The points on the plot are not curve-forming. The chaotic regions are located near the two heteroclinic fixed points where the unstable manifold and stable manifold intersect many times. This is clearly demonstrated in Fig. 3 for a local region near the upper heteroclinic point with higher resolution. Previous studies on this subject can be found in Refs. [9,10]. If the space-charge parameter is reduced to $s_b = 0.6$, and the bunch length is kept the same, the particle dynamics for particles with the same energy and canonical angular momentum becomes much more regular. From the Poincaré plot shown in Fig. 4, there are no detectable islands or chaotic regions over scale lengths comparable to the bunch size and particles' thermal velocity. Chaotic regions with smaller scale-length may still exist, because the particle dynamics is nonintegrable for $s_b > 0$. However, the result in Fig. 4 indicates that for moderately high-intensity beams, a good approximate invariant exists in addition to the exact invariants of energy and canonical angular momentum. This approximate invariant can be used to construct approximate kinetic equilibria with anisotropic energy.

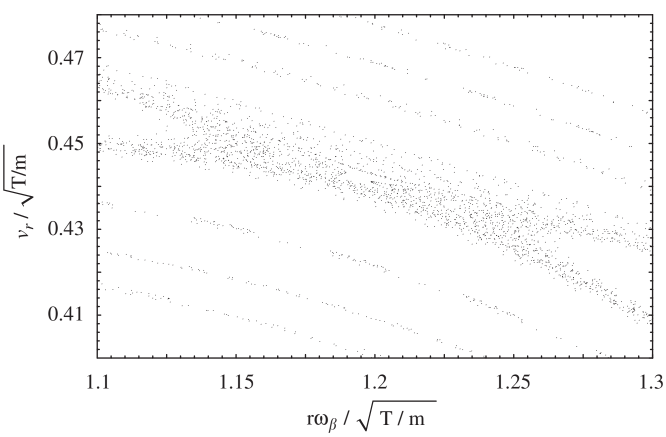

Fig. 3. Expanded region of Fig. 2 near the upper heteroclinic point.

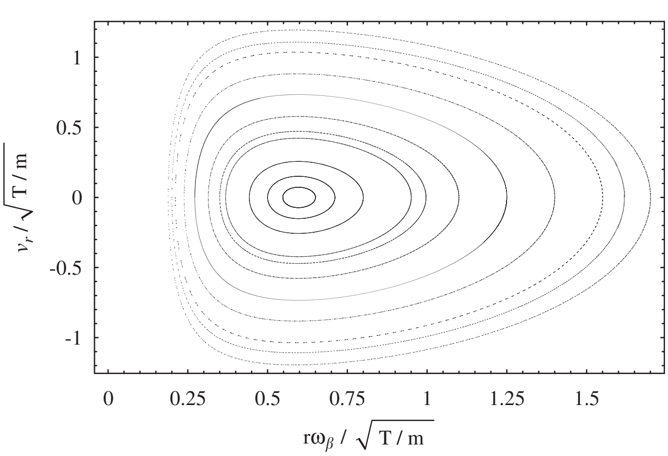

Fig. 4. The $r{-}v_r$ Poincaré plot at $z = 0$ with constant energy and angular momentum in a bunched beam with $s_b = 0.6$.

Once the equilibrium is determined, we can apply the δf particle simulation method to examine the linear and nonlinear evolution of perturbations in the system. In the present paper, we focus only on linear (small-amplitude) perturbations. Because the particles' unperturbed orbits are nonintegrable, it is impossible to carry out the conventional analytical procedure of integrating along unperturbed orbits in an eigenmode calculation. From the point of view of particle simulations, the nonintegrability does not present any difficulty. Linear perturbations can be simulated in the same way as for coasting beams, where the particles' unperturbed orbits are integrable. Numerically, a small-amplitude initial perturbation is imposed at $t = 0$, and the system is evolved using the δf method.

As a demonstration, let's consider a beam with $s_b = 0.27$ and $v_{th}/c = 1.6 \times 10^{-3}$, and $r_w\omega_\beta/c = 6.75 \times 10^{-3}$. Shown in Figs. 5–7 is the oscillation spectrum of the perturbed

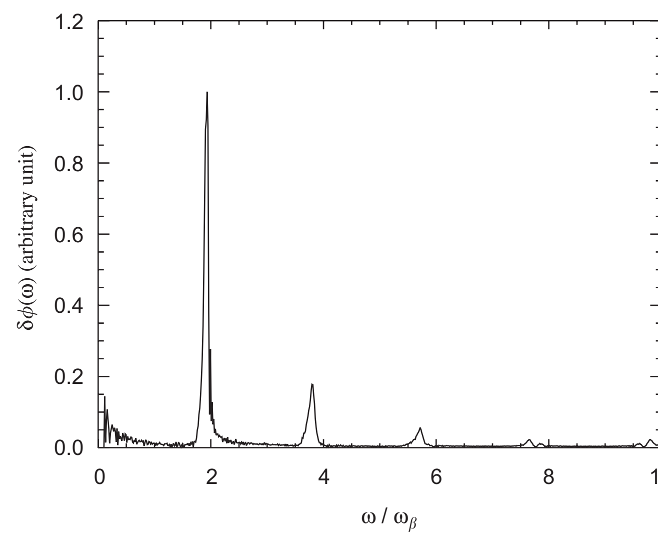

Fig. 5. Spectrum of perturbations at $(r/r_b, z/r_b) = (0.2, 0)$ for $z_b/r_b = 100$.

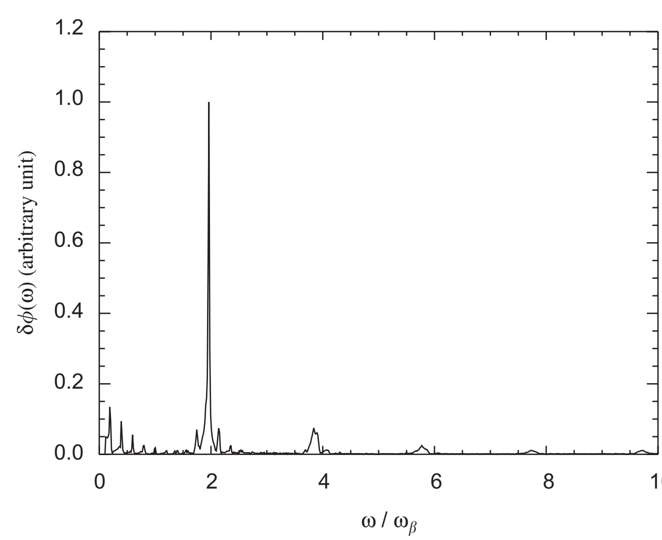

Fig. 6. Spectrum of perturbations at $(r/r_b, z/r_b) = (0.2, 0)$ for $z_b/r_b = 10$.

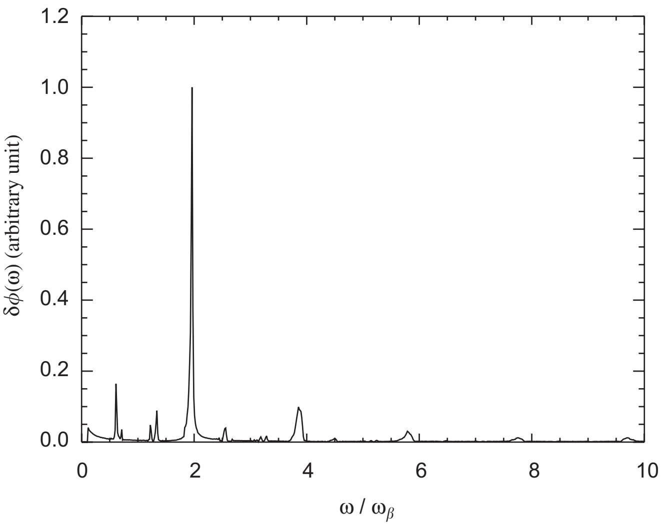

Fig. 7. Spectrum of perturbations at $(r/r_b, z/r_b) = (0.2, 0)$ for $z_b/r_b = 3$.

potential $\delta\phi$ at $(r/r_b, z/r_b) = (0.2, 0)$ for different bunch length. Here, r_b and z_b are rms beam size in the transverse and longitudinal directions defined as

$$r_b^2 = \frac{\int_0^{r_w} r^3 n(r,0)\,dr}{\int_0^{r_w} rn(r,0)\,dr} \tag{20}$$

$$z_b^2 = \frac{\int_0^{\infty} z^2 n(0,z)\,dz}{\int_0^{\infty} n(0,z)\,dz}. \tag{21}$$

The distinguished eigenfrequencies located near $\omega_r = 2\omega_\beta$, $4\omega_\beta$, $6\omega_\beta, \ldots$ are the transverse body modes, which are relatively insensitive to the bunch lengths. For the case where $z_b/r_b = 100$, the spectrum is essentially identical to that of a coasting beam, which has been previously studied both numerically and analytically [1]. As the bunch length decreases, we observe collective mode excitations at additional frequencies (see Figs. 6 and 7). These modes are generated by the coupling of the transverse and longitudinal dynamics, and are most prominent for the case where $z_b/r_b = 3$. For long bunched beams, there is a clear separation of time scales for the transverse and longitudinal dynamics and the coupling becomes less significant. The finite width of the peaks in the spectra that are plotted corresponds to the fact that the eigenmodes are damped. From Figs. 5–7, the eigenmode near $\omega_r = 2\omega_\beta$ is more heavily damped for the case with $z_b/r_b = 100$.

4. Collective excitations for bunched beams with energy isotropy

To model bunched beams in accelerators, it is desirable to consider equilibria with anisotropic energy in the transverse and longitudinal directions. However, as discussed previously, such exact kinetic equilibria do not exist for bunched beams because of the fact that the transverse energy and longitudinal energy are not conserved separately due to the coupling induced by the space-charge field. Approximate kinetic equilibria with anisotropic energy can be constructed for long bunches, or other cases where the coupling induced by the nonlinear space-charge field is weak. For these cases, the transverse energy $H_\perp$ and longitudinal energy H_z defined by

$$H_\perp = \frac{p_\perp^2}{2m} + \frac{m}{2}\omega_\beta^2 r^2 + e\widetilde{\phi_0}(r,z) \tag{22}$$

$$H_z = \frac{p_z^2}{2m} + \frac{m}{2}\omega_z^2 z^2 + e\langle\phi_0\rangle(z) \tag{23}$$

are approximately conserved. Here, $\langle\phi_0\rangle$, $\widetilde{\phi_0}$, and $\overline{\phi_0}$ are defined by

$$\langle\phi_0\rangle(z) = \overline{\phi_0}(z) - \overline{\phi_0}(0) \tag{24}$$

$$\widetilde{\phi_0}(r,z) = \phi_0(r,z) - \langle\phi_0\rangle(z) \tag{25}$$

$$\overline{\phi_0}(z) = \frac{\int_0^{r_w} r\phi_0(r,z)\,dr}{r_w^2/2}. \tag{26}$$

As an example, we choose the reference distribution function f_0 to be

$$f_0 = \frac{\hat{n}}{(2\pi m T_\perp)(2\pi m T_z)^{1/2}} \exp\left(-\frac{H_\perp}{T_\perp} - \frac{H_z}{T_z}\right). \tag{27}$$

Here, $T_\perp$ and T_z are the transverse and longitudinal temperatures, respectively. In the present study, we assume that $T_\perp$ and T_z are time-independent when the reference state is slowly evolving. Of course, the temperature anisotropy is a source of instability [8], which is not being considered in this model. The reference density profile n_0 and reference potential ϕ_0 are determined self-consistently from Eq. (10).

There are two terms that determine the dynamics of w in Eq. (5). The $(df_0/dt)_\delta$ term is explicitly related to the perturbed fields, and the second $(df_0/dt)_0$ term is related to the fact that the reference state f_0 is not an exact solution of the Vlasov–Maxwell equations. To carry out the δf particle simulations, we need to calculate the $(df_0/dt)_0$ term first. Some straightforward algebra gives

$$\frac{1}{f_0}\left(\frac{df_0}{dt}\right)_0 = -\frac{\dot{H}_\perp}{T_\perp} - \frac{\dot{H}_z}{T_z} = \dot{H}_z\left(\frac{1}{T_\perp} - \frac{1}{T_z}\right) \tag{28}$$

$$\dot{H}_z = e\dot{z}\frac{\partial\widetilde{\phi_0}(r,z)}{\partial z}. \tag{29}$$

When the simulation is carried out without an initial perturbation relative to the reference state, the perturbed dynamics simulated gives the beam evolution relative to the reference state. Typical results are shown in Fig. 8 for the perturbed potential at a fixed location in a charge bunch with $s_b = 0.27$, $\sqrt{T_\perp/mc^2} = 1.6 \times 10^{-3}$, $T_z/T_\perp = 0.1$, and $z_b/r_b = 10$. The perturbed quantities $(\delta f, \delta\phi)$ can be viewed as the leading-order description of a quiescent beam, which is referred as a dynamic equilibrium in the present study. Because the perturbed fields are generated

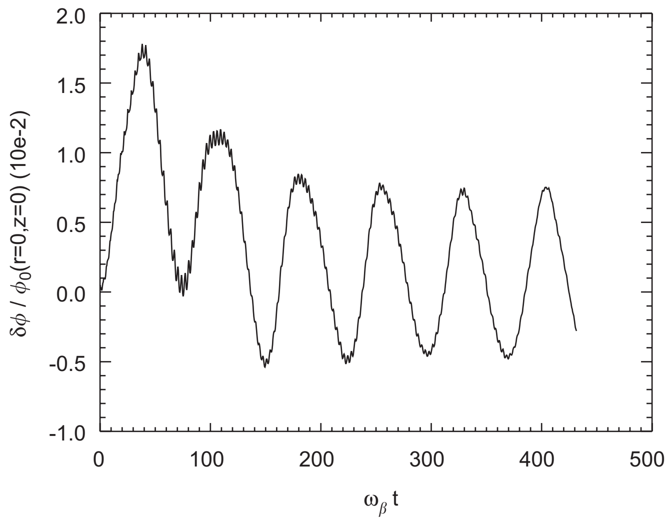

Fig. 8. The perturbative particle simulation establishes the dynamic equilibrium.

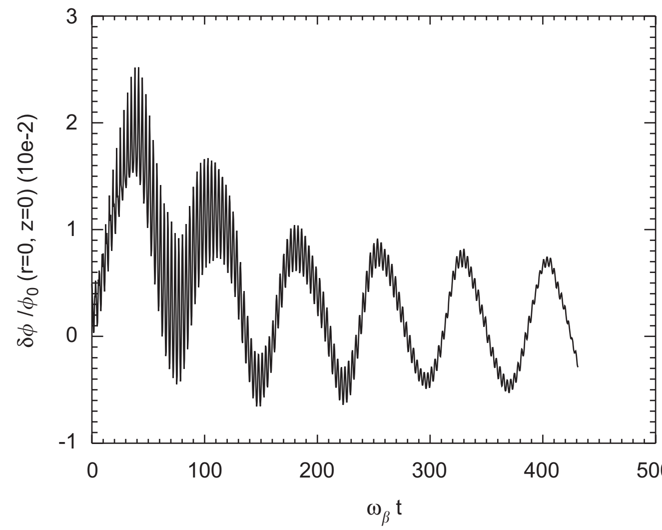

Fig. 9. Time history of the perturbed potential at a fixed spatial location shows collective excitations relative to the dynamic equilibrium.

by both the $(\mathrm{d}f_0/\mathrm{d}t)_0$ term and the initial perturbation, the perturbed fields will be dominated by $(\mathrm{d}f_0/\mathrm{d}t)_0$ when the initial perturbation is small. To utilize the low noise advantage provided by the δf-method, we need to construct a reference state which is a relatively good approximation to an equilibrium such that the perturbed field produced by $(\mathrm{d}f_0/\mathrm{d}t)_0$ is small. In the examples demonstrated in this paper, the typical fluctuation level generated by $(\mathrm{d}f_0/\mathrm{d}t)_0$ is less than 5%. When an initial perturbation is introduced relative to the dynamic equilibrium, we observe collective excitations relative to the dynamic equilibrium, which is illustrated in Fig. 9. The spectrum of the perturbed potential $\delta\phi$ is shown in Fig. 10, from which we conclude that the high-frequency component of the perturbed potential is almost identical to that shown in Fig. 6. By comparing Figs. 9 and 8, it is evident that the perturbed fields for these two cases have similar low-frequency components. Clearly, there is a natural separation of scale-lengths in time for the collective excitation and the dynamic equilibrium. For the collective excitations, the dynamic equilibrium provides a slowly evolving background. Another phenomena demonstrated in Fig. 9 is that the high-frequency component of $\delta\phi$ is damped, which is consistent with the result shown in Fig. 6 as discussed in Section 3.

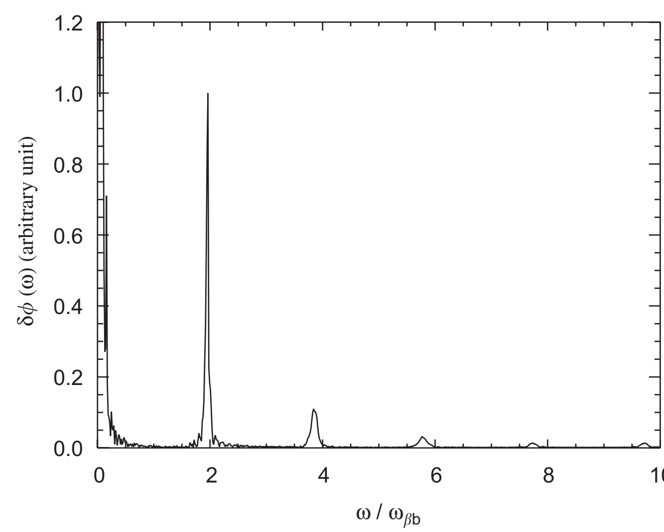

Fig. 10. Spectrum of perturbations at $(r/r_b, z/r_b) = (0.2, 0)$ for $z_b/r_b = 10$ and $T_z/T_\perp = 0.1$.

5. Conclusions

Collective effects with strong coupling between the longitudinal and transverse dynamics are of fundamental importance for applications of high-intensity bunched beams. In the present study, we have applied the nonlinear Vlasov–Maxwell equations to this interesting topic, and developed a generalized δf particle simulation method for high-intensity bunched beams with or without energy anisotropy. Systematic studies were carried out for the particle dynamics under strong 3D nonlinear space-charge forces. The simulations showed that finite-bunch-length effects on collective excitations are not significant when the aspect ratio (z_b/r_b) is larger than 10 for a moderately intense beam with space charge intensity $s_b = 0.27$. For bunched beams with energy anisotropy, a reference state was constructed and the dynamical equilibrium was established in the simulations. Collective excitations relative to the dynamic equilibrium have also been successfully simulated by the generalized δf algorithm.

References

[1] R.C. Davidson, H. Qin, Physics of Intense Charged Particle Beams in High Energy Accelerators, World Scientific, Singapore, 2001.

[2] H. Qin, Phys. Plasmas 10 (5) (2003) 2078.

[3] R.C. Davidson, Phys. Rev. Lett. 81 (1998) 991.
[4] H. Qin, E.A. Startsev, R.C. Davidson, Phys. Rev. ST Accel. Beams 6 (1) (2003) 014401.
[5] H. Qin, R.C. Davidson, W.W. Lee, Phys. Rev. ST Accel. Beams 3 (2000) 084401.
[6] R.C. Davidson, H. Qin, P.H. Stoltz, T.S. Wang, Phys. Rev. ST Accel. Beams 2 (1999) 054401.
[7] E.A. Startsev, R.C. Davidson, H. Qin, Phys. Plasmas 9 (2002) 3138.
[8] E.A. Startsev, R.C. Davidson, H. Qin, Phys. Rev. ST Accel. Beams 6 (2003) 084401.
[9] C. Bohn, I. Sideris, Phys. Rev. ST Accel. Beams 6 (2003) 034203.
[10] S.R. Hudson, H. Qin, R.C. Davidson, Nucl. Instr. and Meth. A 544 (2005) 458.